



SCUOLA INTERNAZIONALE SUPERIORE DI STUDI AVANZATI

SISSA Digital Library

Myoblast adhesion, proliferation and differentiation on Human Elastin-Like Polypeptide (HELP) hydrogels

This is the peer reviewed version of the following article:

*Original*

Myoblast adhesion, proliferation and differentiation on Human Elastin-Like Polypeptide (HELP) hydrogels / D'Andrea, P.; Civita, D.; Cok, M.; Severino, L. U.; Vita, F.; Scaini, Denis; Casalis, L.; Lorenzon, P.; Donati, I.; Bandiera, A.. - In: JOURNAL OF APPLIED BIOMATERIALS & FUNCTIONAL MATERIALS. - ISSN 2280-8000. - 15:1(2017), pp. 43-53.

*Availability:*

This version is available at: 20.500.11767/33173 since:

*Publisher:*

*Published*

DOI:10.5301/jabfm.5000331

*Terms of use:*

openAccess

Testo definito dall'ateneo relativo alle clausole di concessione d'uso

*Publisher copyright*  
SAGE Publishing

This version is available for education and non-commercial purposes.

(Article begins on next page)

Myoblasts adhesion, proliferation and differentiation on  
Human Elastin-Like Polypeptide (HELP) hydrogels

Short title: Myoblasts on Human Elastin-Like Polypeptide (HELP) hydrogels

Paola D'Andrea<sup>1\*</sup>, Deborah Civita<sup>1</sup>, Michela Cok<sup>1</sup>, Luisa Ulloa Severino<sup>1,2</sup>, Francesca Vita<sup>1</sup>, Denis Scaini<sup>1,2</sup>, Loredana Casalis<sup>2</sup>, Paola Lorenzon<sup>1,3</sup>, Ivan Donati<sup>1</sup> and Antonella Bandiera<sup>1</sup>

<sup>1</sup> Department of Life Sciences, University of Trieste, I-34127, Trieste, Italy

<sup>2</sup> NanoInnovation Lab at ELETTRA Synchrotron Light Source S.S. 14 km 163.5, 34012 Basovizza (Trieste), Italy

<sup>3</sup> Centre for Neuroscience B.R.A.I.N., University of Trieste, I-34127, Trieste, Italy

\*Corresponding Author

Department of Life Sciences,  
University of Trieste,  
Via Licio Giorgieri n.1  
I-34127, Trieste, Italy  
Fax 0039 40 5583691  
E-mail address: [dandrea@units.it](mailto:dandrea@units.it)

Figures: 6

Supplemental figures: 1

Word counts: 4917

## ABSTRACT

**Purpose:** The biochemical, mechanical and topographic properties of extracellular matrix are crucially involved in determining skeletal muscle cells morphogenesis, proliferation and differentiation. Human elastin-like polypeptides (HELPS) are recombinant biomimetic proteins designed to mimicking some properties of the native matrix protein; when employed as myoblasts adhesion substrates they stimulate *in vitro* myogenesis. Given the consequences that biophysical properties of extracellular matrix exert on skeletal muscle cells, the aim of this work was to investigate the effects of HELP hydrogels on myoblasts viability and functions.

**Methods:** We recently synthesized a novel polypeptide, HELPc, by fusing the elastin-like backbone to a 41aa stretch present in the  $\alpha 2$  chain of type IV collagen, containing two RGD motifs. To obtain hydrogels, the enzymatic cross-linking of the HELPc was accomplished by transglutaminase. Here, we employed both non cross-linked HELPc glass coatings and cross-linked HELPc hydrogels at different monomer density as adhesion substrates for C2C12 cells, used as myoblasts model.

**Results:** By comparing cell adhesion, proliferation and differentiation, we revealed several striking differences. Depending on support rigidity, adhesion to HELPc substrates dictates cell morphology, spreading, focal adhesions formation and cytoskeletal organization. Hydrogels greatly stimulated cell proliferation, particularly in low serum-medium, and partially inhibited myogenic differentiation.

**Conclusions:** In the whole, the results underline the potentiality of these genetically engineered polypeptides as a tool for dissecting crucial steps in myogenesis.

### Keywords:

Elastin-like polypeptides

Biomimetic materials

Hydrogel

Cell adhesion

Myogenesis

## 1. INTRODUCTION

Eukaryotic cells have the capacity of sensing and decoding not only the chemical composition of the extracellular matrix (ECM) but also its physical properties such as dimensionality, stiffness, and architecture [1-3]. Moreover, there is now much evidence that several pathologies, such as cardiomyopathies, atherosclerosis, muscular dystrophies and cancer are associated with alterations in both the chemical and mechanical properties of the ECM [4]. Accordingly, scaffolds and matrices are increasingly employed in soft tissue engineering due to their ability to support cell survival and activity, acting both as a mechanical support and as cell interactors and modulators [5]. Compared to their natural counterparts, ECM proteins obtained by recombinant DNA technology have intrinsic advantages, including reproducible macromolecular composition, sequence and molecular mass, and overcoming the potential pathogens transmission related to polymers of animal origin [6]. Recombinant elastin-like polypeptides are modeled after the aminoacid sequence of the native elastin, an abundant ECM protein, which plays a pivotal role in tissue biomechanical properties and modulates a variety of cellular responses [7; 8]. In our laboratory, synthetic genes based on the repeated hexapeptidic motifs that characterize human tropoelastin have been cloned and expressed, and the resulting recombinant proteins, Human Elastin-Like Polypeptides (HELPS), have been described and characterized [9;10]. Three of these polypeptides, employed as adhesion substrates for C2C12 myoblasts, stimulate *in vitro* myogenesis to a different extent, strictly dependent on their primary structure [11]. Among the HELP family of polypeptides, both the prototype, HELP [12], and the novel, fusion peptide HELPc [11] contain a repetitive, hydrophilic sequence accommodating Gln and Lys residues which can be enzymatically cross-linked, giving rise to hydrogel matrices [13; 14]. To exploit the potential advantages of HELP-based hydrogels on myoblasts functions, we cultured C2C12 cells on HELPc hydrogels at different monomer concentration, with the aim to couple the biochemical properties of HELPc polypeptide with the mechanical features of hydrogels. By comparing the responses of C2C12 cells seeded on HELPc hydrogels or on non cross-linked HELPc glass coatings we found some intriguing differences in cell adhesion, morphology, proliferation and

differentiation, indicating that HELPc hydrogels can be employed as tools for testing the physiological consequences of cell-biomaterial interactions.

## 2. METHODS

### 2.1 Reagents, antibodies and fluorochromes

Unless otherwise stated, reagents were purchased from Sigma-Aldrich (St. Louis, MO). Bacterial transglutaminase (TGase), from *Streptomyces mobaraensis* was supplied by N-Zyme BioTec GmbH. Anti-vinculin antibody (mouse monoclonal, V9131, Sigma-Aldrich, St. Louis, MO) was employed at 1:200 dilution. Antibody against Myosin Heavy Chain (rabbit polyclonal antibody, H-300, Santa Cruz Biotechnology, Santa Cruz, CA) at 1:30 dilution. Alexa Fluor 488-conjugated AffiniPure goat anti-mouse IgG, (Jackson ImmunoResearch Laboratories, West Grove, PA), at 1:100 dilution. Goat anti-rabbit fluorescein isothiocyanate (FITC)-conjugated affinity purified IgG (Jackson ImmunoResearch Laboratories, West Grove, PA) was employed at 1:200 dilution. DAPI (4',6-diamidino-2-phenylindole, Sigma-Aldrich) was employed at 100 ng/ml. Alexa Fluor 594 phalloidin (Molecular Probes, Eugene, OR) was employed at 0.008 U/cover slip.

### 2.2 HELPc synthesis and preparation of cross-linked HELPc hydrogels

The sequence of HELPc is reported in Fig.1a and its synthesis has been previously described [9; 11]. Briefly, the synthetic gene of the HELP polypeptide was fused with the 41aa coding sequence corresponding to the 854-895 region of the collagen IV  $\alpha 2$  chain (NP\_001837.2), exploiting the unique DraIII site in the expression vector that allows the in-frame insertion at the C-terminus of the polypeptide [12]. The final construct was verified by sequencing and the recombinant product was expressed in the C3037 E. coli strain (New England Biolabs, Ipswich, MA). Expression and purification were carried out as described [9]. The recombinant polypeptide obtained was analyzed by SDS-PAGE and the purified product was lyophilized for long term storage. The lyophilized polypeptide was re-dissolved in water and sterilized by filtration (0.22 $\mu$ m). Protein concentration was verified by the Bradford method and adjusted to the desired level by dilution.

Non cross-linked HELPc coatings were obtained by depositing 0.1 mg/ml of aqueous protein solution onto borosilicate glass coverslips; 0.1 ml of coating solution was used per 1 cm<sup>2</sup> surface area, thus resulting in 10 g polypeptide/cm<sup>2</sup>. Coating solution was allowed to dry in a tissue culture hood and

cells were seeded directly on the polypeptide surface. Enzymatic cross-linking was performed in a tissue culture hood under sterile condition. To obtain HELPc hydrogels the polypeptide was cross-linked with bacterial TGase. The recombinant protein, was dissolved in 10mM Tris/HCl, pH 8, to a final concentration of 5% and 7% w/v. Solutions (100 $\mu$ l each) were stored in an ice bath for 30 min to promote solubilization. Subsequently, 0.53U of TGase (133U/ml) were added and the reaction mixture was quickly mixed. 15 $\mu$ l of each polypeptide solution were dropped on round glass coverslips (13mm) and incubated at 10°C for 2h.. Cross-linking was completed after overnight incubation at 4°C. Hydrogels were bathed with 70% ethanol and then rinsed thoroughly with ultra-pure water. Before cell seeding, hydrogels were washed extensively with Phosphate Buffered Saline (PBS).

### *2.3 Rheological analysis and determination of shear modulus*

Rheological measurements were performed on HELPc hydrogel specimens at 5% and at 7%, respectively, under oscillatory shear conditions to determine the extension of the linear viscoelasticity regime (stress sweep tests at 1 Hz) and the mechanical spectra (frequency sweep). The complex viscosity ( $\eta^*$ ), the storage ( $G'$ ), and loss ( $G''$ ) moduli of the hydrogels were recorded in the frequency range 0.01-20 Hz (stress = 4Pa, within the linear regime). All of the tests were carried out with the controlled stress rheometer Rheostress Haake RS 150 operating at 25°C. A serrated plate PP20 Ti was employed for the mechanical spectra of the hydrogels to prevent slippage effects. In the case of the hydrogels, the contact between the serrated plates and the sample was verified through stress sweep tests performed at different gap values, and a 1.2 mm gap was finally selected.

### *2.4 SEM analysis*

Samples of 5% and 7% (w/v) of HELPc hydrogel were prepared as described above (paragraph 2.2) using cylindrical molds (4mm diameter x 4mm high). After hydrogel formation, samples were extensively washed in distilled water, frozen at -20 C and lyophilized. Slices were cut, mounted onto stubs using a double-sided adhesive and sputter coated with gold. Analysis was performed using a Leica Stereoscan 430i Scanning Electron Microscope.

### *2.5 Atomic force microscopy analysis*

AFM was used to characterize HELPc dehydrated hydrogels thickness and morphology. AFM images were acquired using a commercially available microscope (Asylum Research MFP-3D<sup>®</sup> Stand Alone AFM from Oxford Instruments, Santa Barbara, CA ó U.S.) endowed with a 90×90×15  $\mu$ m closed-loop metrological scanner. All AFM measurements were carried out in air at room temperature working in dynamic mode. HELPc hydrogels were carefully washed using milliQ water and gently dried in a nitrogen oven overnight at room temperature. Cantilevers used were characterized by a free resonance frequency of about 65 kHz and a force constant of about 0.6 nN/nm (HQ:NSC36/C from MikroMasch Co. - Tallinn ó Estonia). 512×512 pixels images were acquired at 0.5 lines/second scan speed to assess the morphology of dehydrated hydrogels. Thickness was calculated as height difference between the film upper surface and the underneath glass surface previously exposed by scratching away the gel with a scalpel. Heights were evaluated as mean value of 10 height profiles traced in different positions perpendicularly to a single scratch line. Gwyddion software ([www.gwyddion.net](http://www.gwyddion.net)) was used to analyze AFM images and to compute surface roughness ( $R_a$ ) while all statistics and data processing were performed using Igor Pro software ([www.wavemetrics.com](http://www.wavemetrics.com)).

### *2.6 Cell culture and differentiation protocol*

Mouse myogenic C2C12 cells (ATCC CRL-1772) were maintained as exponentially growing myoblasts in a Growth Medium consisting of Dulbecco's Modified Eagle's Medium (DMEM) supplemented with 20% heat-inactivated fetal calf serum, 4mM L-glutamine, 100IU/ml penicillin and 100  $\mu$ g/ml streptomycin. Cells were cultured on 10cm polystyrene Petri dishes at 37°C in a 5% CO<sub>2</sub> incubator. Cell were serially passed at about 75% confluence every 2-3 days. For adhesion assays, cells were plated at a density of 10<sup>4</sup>cells/cm<sup>2</sup>, and allow adhering for 5h. To obtain cell differentiation and myotube fusion, cells were plated at a density of 5×10<sup>3</sup>cells/cm<sup>2</sup>. 48h after plating, cells were shifted to Differentiation Medium, consisting of DMEM supplemented with 2% heat-inactivated horse serum, 4mM glutamine, 100IU/ml penicillin and 100  $\mu$ g/ml streptomycin.



## *2.7 Immunofluorescence*

The general protocol for immunofluorescence experiments is described. Coverslips were washed three times with PBS and then fixed with 4% paraformaldehyde for 30min at 4°C. After fixation, samples were blocked with a solution containing 5% normal goat serum, 0.1% Triton-X 100 in PBS for 10min. Samples were incubated overnight at 4°C with a primary antibody at the appropriate dilution. After three washes of 10min with PBS plus 0.1% Triton-X 100, coverslips were incubated with the secondary antibody (or other fluorochromes) for 2h at 4°C. Samples, washed three times for 10min with PBS plus 0.1% Triton-X100, were then mounted onto slides and visualized under a Leica DMLS fluorescence microscope (Leica Microsystems, Wetzlar, Germany). Cells were visualized under a Leica DMLS fluorescence microscope (Leica Microsystems, Wetzlar, Germany). Images were acquired with a Leica DC300F camera, coupled to a Leica IM50 acquisition software. Image sizing, cropping and overlay were performed with Adobe Photoshop CC (Adobe Systems Incorporated, San Jose, CA). Image analysis was performed with ImageJ (NIH, Bethesda, MD; <https://imagej.nih.gov/ij/> ).

## *2.8 Cell viability and proliferation.*

Cells were seeded at a density of  $5 \times 10^3$  cells/cm<sup>2</sup> on 13 mm glass coverslips which were either coated with HELPc or covered with HELPc hydrogels; coverslips were then placed in 24-well plate multi-wells. 48h after plating, cells were shifted to Differentiation Medium. Measurements were performed at 5, 24, 48 and 72h after plating. Cell proliferation was evaluated by nuclei counting. Samples were fixed with 4% paraformaldehyde for 30min at 4°C and then processed for nuclei staining using DAPI at the final concentration of 100ng/ml. Nuclei were counted with ImageJ software. Cell viability was evaluated with the WST-1 (2-(4-iodophenyl)-3-(4-nitophenyl)-5-(2,4-disulfophenyl))-2H-tetrazolium monosodium salt, provided in a pre-mix electro-coupling solution (Roche Applied Science, Mannheim, Germany) according to the manufacturer's instructions.

### *2.9 Differentiation assays*

C2C12 cells were induced to differentiate and, at 5 days, processed for immunofluorescence against Myosin Heavy Chain (MHC). A cell containing 3 or more nuclei was considered as a myotube. The total number of nuclei and of MCH-positive myotubes was counted in 10 random fields (>400 total nuclei) for each condition. The fusion index was calculated as the ratio of the nuclei number in MCH-positive myotubes versus the total number of nuclei in the field. The average number of nuclei per myotube was also determined.

### *2.10 Statistical analysis*

Data were analyzed with OriginPro software (7.5, OriginLab Corp. Northampton, MA). Statistical significance was determined using one-way ANOVA analysis after Levene's test for homogeneity of variances, and followed by the Scheffé test for multiple comparison test. Unless otherwise stated, results were expressed as mean  $\pm$  standard deviation (SD). Difference with  $p < 0.05$  was considered as statistically significant.

### 3. RESULTS

#### 3.1 Properties of HELPc hydrogels.

The sequence scheme of HELPc is reported in Fig.1a. The elastin-like backbone of the polypeptide is fused, at the C-terminus, with a 41aa stretch from collagen type IV  $\alpha 2$  chain isoform, allocating two RGD motives. The polypeptide was designed to genetically encode hydrophilic domains containing glutamine and lysine residues which can undergo enzymatic cross-linking by transglutaminase [12; 13]. Accordingly, the Ala-rich, hydrophilic sequence of the elastin-like polypeptides containing the Lys and Gln residues is also called the "cross-linking domain" [15]. Concentrations of 5 and 7% w/v were selected as optimal for the cross-linking reaction because lower concentrations (4%) failed to generate stable hydrogels, whereas concentrations higher than 7% w/v tended to give solubility problems, as previously described [13]. Indeed, a peculiar and well known property of elastins (both natural and recombinant) is coacervation (or "self assembly"); under appropriate conditions of concentration, ionic strength and temperature, the protein separates from the solution as a second phase [16].

Rheological measurements under oscillatory shear were performed to characterize HELPc hydrogels. Figure 1b reports the mechanical spectrum of the HELPc hydrogels at the concentration of 5% and 7%, respectively. It can be noticed the elastic modulus of the 5% hydrogel is markedly lower (one order of magnitude) than that of the 7% hydrogel. However, in both cases  $G'$  is higher than  $G''$  and shows little variation within the pulsation range explored. For the sake of comparison, a non-calcium saturated 1.5 % alginate hydrogel shows an elastic modulus which is approximately one order of magnitude higher than the one displayed by the 7 % HELPc sample [17].

The frequency sweep test were interpreted in terms of the generalized Maxwell model composed of a sequence of elements in parallel (spring and dashpot) to which an additional spring has been added [18]. The storage and loss moduli can be modeled as a function of the pulsation according to the following equations (eqs 1 and 2):

$$G'(\omega) = G_{\infty} + \sum_{i=1}^n G_i \frac{\omega^2 \tau_i^2}{1 + \omega^2 \tau_i^2} \quad \text{eq. 1}$$

$$\sigma = \sum_{i=1}^n \frac{G_i \epsilon}{1 + i \tau_i \dot{\epsilon}} \quad \text{eq. 2}$$

where  $n$  is the number of Maxwell elements considered,  $G_i$ ,  $\tau_i$ , and  $i$  represent the spring constant, the dashpot viscosity, and the relaxation time of the  $i$ th Maxwell element, respectively.  $G_e$  is the spring constant of the last Maxwell element which is supposed to be purely elastic. The fitting of the experimental data was performed assuming that relaxation times are not independent each other but they are scaled by a factor 10. Hence, the parameters of the model are  $G_e$ ,  $\tau_i$ , and  $i$ . The number of the Maxwell elements was selected, based on a statistical procedure, to minimize the product  $\chi^2 * N_p$ , where  $\chi^2$  is the sum of the squared errors, while  $N_p (=2+n)$  indicates the number of fitting parameters.

The use of a generalized Maxwell model allowed determining the shear modulus,  $G$ , as (eq. 3)

$$G = G_e + \sum_{i=1}^n G_i \quad \text{eq. 3}$$

For the 7% HELPc hydrogel  $G$  was calculated to be  $512 \pm 28$  Pa, while it is reduced to  $63 \pm 12$  Pa when the 5% HELPc hydrogel is considered. As a comparison, a calcium-saturated 1% alginate hydrogel showed a  $G$  of approximately 55 kPa [17].

The SEM analysis of cross-sectional interior structures of lyophilized HELPc hydrogels is shown in Fig.1c. Both 5% and 7% matrices exhibited a porous honeycomb-like structure with an irregular shape in which the three-dimensional, interconnected macro-pores represent water-filled areas, while the pore size depends on monomer concentration. Specifically, the hydrogels at 5% HELPc were characterized with an average pore diameter of  $227 \pm 36.6$   $\mu\text{m}$  ( $n=50$ ), while 7% ones exhibited much denser structure with an average pore size of  $74 \pm 32.5$   $\mu\text{m}$  ( $n=56$ ;  $p < 0.001$ ).

HELPC hydrogels appeared opaque and wax-like at visual inspection (Supplemental Fig.1a). The different compactness of the two matrices was highlighted when hydrogels were casted in cylindrical molds. As shown in Supplemental Fig. 1b, after removing the excess of water, the 7% hydrogel retained its shape, whereas the 5% tended to collapse. The hydrogels surfaces, observed under phase contrast microscope, appeared uniform, smooth and crossed by several folds (Supplemental Fig. 1c), presumably resulting from shrinkage during the cross-linking process.

Atomic Force Microscopy (AFM) was employed to characterize some properties HELPC hydrogels.

Preliminary attempts to determine the morphology and the mechanical properties of HELPC

hydrogels by AFM revealed unsuccessful given that the different probes employed for indentation tests tended to stick to the hydrogel surfaces (in particular to tips characterized by large contact surface, such as sphere-endowed cantilevers), thus preventing the measures of hydrogel morphology and elastic modulus. To partially overcome this problem, obtaining anyway a preliminary characterization of the two HELPc-based matrices, surface texture, morphology and thickness were evaluated on dehydrated hydrogels (DH). AFM images of DH surfaces (Supplemental Fig. 1d) reveal similar clouded morphology for the two samples, which appeared substantially different from the previously reported grainy and uneven distribution of non-crosslinked HELPc coatings [11]. The roughness of 5% one ( $R_a$  about 60.8 nm) was slightly higher than 7% sample ( $R_a$  about 32.5 nm). DHs height profile measurements over a till-glass scratch (see Methods) reveal that 7% samples were significantly thicker than 5% ( $3.702 \pm 1.431 \mu\text{m}$  versus  $1.583 \pm 0.446 \mu\text{m}$ ,  $p < 0.01$ ). This is likely due to the higher cross-linking level of 7% DH.

### 3.2 Cell adhesion

Adhesion and spreading of C2C12 cells were evaluated 5h after seeding on 5% and 7% HELPc hydrogels. Adhesion properties were compared to those exhibited by the same cells adhering on HELPc coatings (Hcc) obtained by adsorbing the polypeptide to glass coverslips [11]. The stability of non-crosslinked HELP polypeptides adsorbed to plastic or to glass coverslips has been previously assessed by X-ray photoelectron spectroscopy [21] and by immunofluorescence and AFM [11]. By immunostaining vinculin to visualize cell cytoplasm and focal adhesions, several morphological and functional differences could be observed (Fig. 2). Cells seeded on HELPc coating appeared flattened, well spread and displaying, in many cases, wide lamellipodia (Fig. 2a). On 5% hydrogels most myoblast appeared stellate due to protrusions expanding in all directions and often branching. Myoblast adhering on 7% hydrogels mostly displayed an elongated and polarized morphology, characterized by a fan-like shape and a long trailing edge. The histogram distribution of cell aspect ratio and area accounts for the heterogeneity of cell populations, and highlights the differences observed in Fig.2a. Cell aspect ratio (AR) is an assessment of cell morphology, being the ratio

between the length of the major axis to the minor axis of a single cell. Accordingly, the more elongated the cell, the higher the AR, whereas a polygonal cell exhibits an AR close to 1. Cells seeded on HELPc coating show the prevalence of polygonal-circular shape and a considerable degree of spreading (area). Cells seeded on 5% hydrogels spread less on the substrate and their aspect ratio values indicates a more elongated morphology. Conversely, cells seeded on 7% hydrogels show a broader distribution of both aspect ratio and cell area, with a considerable fraction of the cell population showing an increased length and a higher degree of spreading.

Given the role of cytoskeleton in shaping cell morphology and the part played by vinculin in coordinating the focal adhesion network and organizing the actin cytoskeleton dynamics [22], we compared f-actin organization and vinculin distribution 5h after seeding (Fig.3). Cells seeded on HELPc coating were characterized by a highly organized actin meshwork with numerous stress fibers intersecting and ending at focal adhesions, suggesting a state of isometric contraction [23]. Vinculin staining showed marked elongated spots, distributed not only at the cell periphery, but scattered throughout the cell soma, indicating an organized network of focal adhesions. Centrally located in the cell body, fibrillar adhesions were also detectable. In cells adhering to 5% hydrogels, the network of actin filaments appeared less defined, with stress fibers running along the main cell axis and ending at the terminals of cell protrusions. Vinculin localized both in the cytosol, where it appeared diffusely distributed, and at the cell membrane, where dotted and dashed spots decorated the cell margins in correspondence of the ending of protrusions, forming focal contacts and small focal adhesions. Cells adhering on 7% hydrogels were characterized by a tightly organized actin meshwork with abundant stress fibers running along the whole cell soma. The thin trailing edge was also rich in filamentous actin. Vinculin staining showed a marked enrichment in elongated spots, distributed both at the cell periphery and throughout the cell soma, indicating a diffuse and organized network of focal adhesions.

### *3.3 Cell viability and growth*

The inhibition of cell proliferation is required for myogenesis to occur [24]. Accordingly, we quantified cell viability and turnover before and after addition of Differentiation Medium (DM). After the initial growth phase in Growth Medium (GM), sampled at 5, 24 and 48h after cell seeding, cells were switched to DM and cultured for another day (72h after seeding). At these time points, in fact, cell-to-cell fusion has not yet started and poly-nucleated cells are not detectable. Cell turnover was evaluated by counting the cell nuclei stained with DAPI (Fig.4a) and by measuring cells metabolic activity with WST-1 (Fig.4c). Fig.4a shows the number of nuclei at the different time points for each culture condition. After 5h the number of cells adhering to the three substrates was not significantly different, even though a tendency to higher adhesion was observed for the Hcc (Hcc  $110 \pm 31$  cells; 5% hydrogels  $90 \pm 37$  cells; 7% hydrogels  $77 \pm 23$  cells). At 24h the number of cells on either sample increased, indicating that proliferation started early after seeding. Moreover, the cell number present on both hydrogels was significantly higher than that present on Hcc. At 48h proliferation continued maintaining the difference between Hcc and hydrogels. At this time the culture medium was shifted to DM, thus lowering by tenfold the concentration of growth factors. 72h after seeding the most striking differences were observed among the different culture conditions. A considerable increase in cell number was observed for cells grown on hydrogels, while the number on Hcc increased to a far lesser extent. To provide a more dynamical description of such variations we calculated, for the three culture conditions, the proliferation rate, by normalizing the nuclei numbers to the initial density (Fig.4b). Compared to cells seeded on Hcc, myoblasts cultured on both hydrogels showed a higher growth rate already at 24 and 48h. Strikingly, the shift to DM boosted proliferation of cells growing on hydrogels, but failed to affect the growth rate on HELPc coating. Similar results were obtained by measuring the cell metabolic activity with the WST-1 assay (Fig.4c,d).

### *3.4 Myotubes differentiation*

During differentiation, the C2C12 cells align and fuse together to form myotubes. To compare the effect of the three HELPc substrates on myogenic differentiation, C2C12 cells were shifted to a low serum medium (Differentiation Medium) to promote the myotube formation. Using phase contrast

microscopy, morphological changes were compared at 5 days of differentiation (Fig.5a). Although a diffuse network of elongated cells was present in all conditions, myotubes developed on Hcc appeared longer and wider with respect to those formed on both 5% and 7% hydrogels, and the first signs of branched structures could be observed. By comparing the morphology of myotubes formed on hydrogels, we noticed that longer and wider myotubes tended develop on 7% gels. After 5-6 days of differentiation, cells started to clump and detach from hydrogels, whereas myotubes developed on Hcc tended to peel off after 9 days, presumably due to spontaneous contractions.

During differentiation of C2C12 cells, the newly formed myotubes express several differentiation markers, among which the muscle-type Myosin Heavy Chain (MHC) is considered one of the latest [25]. Hence, we investigated the expression of MHC at 5 day of differentiation, performing a qualitative and quantitative analysis by indirect immunofluorescence (Fig.5b). Myotubes formed on Hcc appeared long, multinucleated and often branched, due to multiple events of cell-to-cell fusion. Compared to cells adhering to 5% hydrogels, myotubes developed on 7% hydrogels appeared wider and more multinucleated. To quantitatively compare the differences observed in immunofluorescence images, we calculated the fusion index (Fig.5c) and the average number of nuclei in MHC-positive myotubes (Fig.5d). The fusion index represents the ratio of the nuclei number in MCH-positive myotubes (containing at least three nuclei) versus the total number of nuclei in the field. As shown in Fig.5c, the fusion index of myotubes grown on Hcc was considerably higher ( $49.0 \pm 8.5$  %) than that of cells grown on either hydrogel. However, the comparison of fusion index of myotubes developed on hydrogels revealed that it was greater in cells grown on 7% hydrogels (7% hydrogels:  $4.3 \pm 1.0$  %; 5% hydrogels:  $2.4 \pm 0.7$  %). The number of nuclei per myotube (Fig. 5d) was higher for Hcc ( $32.0 \pm 4.7$  nuclei). However, as shown by Fig.5b, also the number of nuclei present on myotubes developed on 7% hydrogels was elevated ( $19.0 \pm 4.0$  nuclei) and significantly higher than that present on 5% hydrogels ( $8.0 \pm 3.0$  nuclei). The morphometric analysis of myotubes developed on the different culture conditions is reported in Fig.6. Myotubes developed on Hcc (Fig.6 a-b) were composed by two main populations: one consisting of elongated, thin cells, with many nuclei aligned along the main cell axis; the other comprising shorter and wider cells, highly branched, due to multidirectional



cell-to-cell fusion. The size of myotubes developed on 5% hydrogels is reported in Fig.6c-d; the majority of them showed a length comprised between 100  $\mu\text{m}$  and 200  $\mu\text{m}$  and an average width of 18  $\mu\text{m}$ . Myotube size significantly changed when cells differentiated on 7% hydrogels, with an increase in both length and width. As shown in Fig.6e, an average increase in myotube length (200-300  $\mu\text{m}$ ) and, most of all, an average 2.6-fold increase in width (47  $\mu\text{m}$ , Fig.8f) characterized these cells.

#### 4. DISCUSSION

Human Elastin Like Polypeptides, as non-crosslinked coatings, have been exploited to promote myoblast adhesion proliferation and differentiation [21; 11]. Moreover, they have been successfully employed to improve the contractile activity of C2C12 cells in collagen/HELP composite scaffolds [26]. In this work, the enzymatic cross-linking of a novel polypeptide of the HELP series allowed the generation of hydrogels at different monomer density, capable of supporting myoblast adhesion, proliferation and, to a far lesser extent, differentiation.

The shear modulus of 5% and 7% HELPc hydrogels differ by an order of magnitude, indicating that even a moderate diversity in monomer concentration produced matrices with considerable differences in mechanical properties. Together with the qualitative observation of an evident discrepancy in hydrogels compactness (Supplemental Fig. 1b), this data supports the view that HELPc hydrogels provide myoblastic cells with substrates highly different in their mechanical properties. Accordingly, the differences observed in cells morphology, vinculin clustering and cytoskeletal organization are likely related to the different compliance of the adhesion substrates. Actually, a more organized cytoskeleton and more stable adhesions characterize cells adhering to stiffer or rigid substrates, despite differences in ligand density and long-time elasticity [3;27-29]. Accordingly, the differences we observed in cell morphology, cytoskeleton organization and adhesion properties would likely depend on the different rigidity of the supporting material. In the whole, these results are in good agreement with previous studies testing C2C12 cell adhesion on soft and stiff substrates obtained from polyelectrolyte multilayers [30-32].

The evidence that adhesion to HELPc hydrogels stimulates cell proliferation, particularly in low serum medium, is intriguing and potentially useful for tissue engineering strategies. Indeed, a major problem in muscle cell therapy is the need for a sufficient number of progenitor cells for successful transplantation; as such, *in vitro* expansion of muscle stem cells represents one of the strategies actively pursued [33;34]. If the proliferative effect of HELPc hydrogels would be observed on muscle precursor cells, it would reveal potentially promising for future applications, particularly for the *in vivo* approach of muscle tissue engineering. This strategy prescribes that expansion is directly

followed by transplantation, avoiding myogenic differentiation *in vitro* [35]. The approach revealed successful when applied to muscle stem cells expanded on soft polyethylene glycol-based substrates: it increased cell viability, prevented their differentiation *in vitro*, but maintained their *in vivo* regenerative properties when engrafted in immunodeficient mice [36].

Myotube formation is partially inhibited in cells growing on HELPc hydrogels. Although the expression of myosin heavy chain indicates that myogenesis started in either condition, the low values of fusion index and the reduced size of myotubes revealed that the process could not proceed beyond a certain stage [37] and that myotube development is abnormal. Intriguingly, the extent of inhibition correlated with substrate compliance, with softer 5% hydrogel being more effective in preventing cell-to-cell fusion and myotube formation. Similar results have been reported for C2C12 cells seeded on polyelectrolyte multilayers of different stiffness [28], suggesting that excessively compliant substrates could hamper the latest stages of myotube formation. In conclusion, besides their potential application in tissue engineering, HELPc-based hydrogels could be employed in studies aimed to dissecting the molecular pathways responsible for the transition of proliferating myoblasts to quiescent, fusing myotubes.

## Acknowledgments

The authors declare no conflicts of interests. This work was supported in part by European Regional Development Fund (CB 101) (Cross-border cooperation Program Italy-Slovenia 2007-2013, Trans2care strategic project), and by Beneficentia Stiftung (BEN 2014/125), Vaduz, Lichtenstein.

## REFERENCES

1. Ross AM, Jiang Z, Bastmeyer M, Lahann J. Physical aspects of cell culture substrates: topography, roughness, and elasticity. *Small*. 2012; 8:336-355.
2. Engler AJ, Griffin MA, Sen S, Bönnemann CG, Sweeney HL, Discher DE. Myotubes differentiate optimally on substrates with tissue-like stiffness: pathological implications for soft or stiff microenvironments. *J Cell Biol* 2004a; 166:877-887.
3. Engler A, Bacakova L, Newman C, Hategan A, Griffin M, Discher D. Substrate compliance versus ligand density in cell on gel responses. *Biophys J*. 2004b; 86:617-628.
4. Bonnans C, Chou J, Werb Z. Remodelling the extracellular matrix in development and disease. *Nat Rev Mol Cell Biol*. 2014;15:786-801.
5. Murphy WL, McDevitt TC, Engler AJ. Materials as stem cell regulators. *Nat Mater*. 2014; 13: 547-557.
6. Cai L, Heilshorn SC. Designing ECM-mimetic materials using protein engineering. *Acta Biomater*. 2014; 10:1751-1760.
7. Urry DW, Pattanaik A. Elastic protein-based materials in tissue reconstruction. *Ann N Y Acad Sci* 1997; 831:326-46.
8. MacEwan SR, Chilkoti A. Elastin-like polypeptides: Biomedical applications of tunable biopolymers. *Biopolymers* 2010; 94:606-77.
9. Bandiera A. Assembly and optimization of expression of synthetic genes derived from the human elastin repeated motif. *Prep Biochem Biotechnol* 2010; 40:198-212.
10. Bandiera A, Sist P, Urbani R. Comparison of thermal behavior of two recombinantly expressed human elastin-like polypeptides for cell culture applications. *Biomacromolecules*. 2010; 11:325-65.
11. D'Andrea P, Scaini D, Ulloa Severino L, Borelli V, Passamonti S, Lorenzon P, Bandiera A. *In vitro* Myogenesis induced by Human Recombinant Elastin-Like Proteins. *Biomaterials* 2015; 67: 2406-253.

12. Bandiera A, Taglienti A, Micali F, Pani B, Tamaro M, Crescenzi V, Manzini G. Expression and characterization of human-elastin-repeat-based temperature responsive protein polymers for biotechnological purposes, *Biotechnol Appl Biochem* 2005;42:247-256.
13. Bandiera, A. Transglutaminase-catalyzed preparation of human elastin-like polypeptide-based three-dimensional matrices for cell encapsulation. *Enzyme Microb. Tech.*, 2011, 49, 347-352.
14. Bozzini S, Giuliano L, Altomare L, Petrini P, Bandiera A, Conconi MT, Farè S, Tanzi MC. Enzymatic cross-linking of human recombinant elastin (HELP) as biomimetic approach in vascular tissue engineering. *J Mater Sci Mater Med*. 2011; 22:2641-50.
15. Vrhovski B1, Weiss AS. Biochemistry of tropoelastin. *Eur J Biochem*. 1998; 258:1-18.
16. Urry DW, Haynes B, Harris RD. Temperature dependence of length of elastin and its polypentapeptide. *Biochem Biophys Res Commun*. 1986; 141:749-55.
17. Marsich, E, Borgogna, M, Donati, I, Mozetic, P, Strand BL, Gomez Salvador S, Vittur F, Paoletti, S. Alginate/lactose-modified chitosan hydrogels: a bioactive biomaterial for chondrocyte encapsulation, *J. Biomed. Mater. Res*. 2008; 84A: 364-376.
18. Turco G, Donati I, Grassi M, Marchioli G, Lapasin R, Paoletti S. Mechanical spectroscopy and relaxometry on alginate hydrogels: a comparative analysis for structural characterization and network mesh size determination, *Biomacromolecules* 2011; 12: 1272-1282)
19. Moe ST, Elgsaeter A, Skjåk-Bræk G, Smidsrød O. A new approach for estimating the crosslink density of covalently crosslinked ionic polysaccharide gels, *Carbohydr. Polym* 1993; 20: 263-286).
20. Moresi M, Bruno M. Characterization of alginate gels using quasi-static and dynamic methods, *J. Food. Eng.* 2007; 82: 298-309
21. Ciofani G, Genchi GG, Liakos I, Athanassiou A, Mattoli V, Bandiera A. Human recombinant elastin-like protein coatings for muscle cell proliferation and differentiation, *Acta Biomater*. 2013; 9:5111-21.
22. Carisey A, Ballestrem C. Vinculin, an adapter protein in control of cell adhesion signaling. *Eur J Cell Biol* 2011; 90:157-163.
23. Discher DE, Janmey P, Wang YL. Tissue cells feel and respond to the stiffness of their substrate. *Science* 2005; 310:1139-1143.

24. Bentzinger CF, Wang YX, Rudnicki MA. Building Muscle: Molecular Regulation of Myogenesis.
25. Miller JB. Myogenic Programs of Mouse Muscle Cell Lines: Expression of Myosin Heavy Chain Isoforms, MyoD1, and Myogenin. *J Cell Biol* 1990; 111:1149-1159.
26. Boccafoschi F, Ramella M, Sibillano T, De Caro L, Giannini C, Comparelli R, Bandiera A, Cannas M. Human elastin polypeptides improve the biomechanical properties of three-dimensional matrices through the regulation of elastogenesis. *J Biomed Mater Res A*. 2015; 103:1218-1230.
27. Pelham RJ, Wang YL, Cell locomotion and focal adhesions are regulated by substrate flexibility. *Proc. Natl. Acad. Sci.* 1997; 94; 13661-13665.
28. Georges PC, Janmey PA. Cell type-specific response to growth on soft materials. *J Appl Physiol* 1985. 2005; 98:1547-1553.
29. Saez A, Buguin A, Silberzan P, Ladoux B. Is the mechanical activity of epithelial cells controlled by deformations or forces? *Biophys J*. 2005; 89:L52-54.
30. Ren K, Crouzier T, Roy C, Picart C. Polyelectrolyte multilayer films of controlled stiffness modulate myoblast cells differentiation. *Adv Funct Mater*. 2008; 18:1378-1389.
31. Ren K, Fourel L, Rouvière CG, Albiges-Rizo C, Picart C. Manipulation of the adhesive behaviour of skeletal muscle cells on soft and stiff polyelectrolyte multilayers. *Acta Biomater* 2010; 6: 42386 4248.
32. Gribova V, Gauthier-Rouvière C, Albigès-Rizo C, Auzely-Velty R, Picart C. Effect of RGD functionalization and stiffness modulation of polyelectrolyte multilayer films on muscle cell differentiation. *Acta Biomater*. 2013; 9:6468-6480.
33. Qazi TH, Mooney DJ, Pumberger M, Geissler S, Duda GN. Biomaterials based strategies for skeletal muscle tissue engineering: existing technologies and future trends. *Biomaterials*. 2015; 53:502-21.
34. Ostrovidov S, Shi X, Sadeghian RB, Salehi S, Fujie T, Bae H, Ramalingam M, Khademhosseini A. Stem Cell Differentiation Toward the Myogenic Lineage for Muscle Tissue Regeneration: A Focus on Muscular Dystrophy. *Stem Cell Rev*. 2015; 11: 866-84.
35. McCullen SD, Chow AG, Stevens MM. In vivo tissue engineering of musculoskeletal tissues. *Curr Opin Biotechnol*. 2011; 22: 715-20.

36. Gilbert PM, Havenstrite KL, Magnusson KE, Sacco A, Leonardi NA, Kraft P, Nguyen NK, Thrun S, Lutolf MP, Blau HM. Substrate elasticity regulates skeletal muscle stem cell self-renewal in culture. *Science*. 2010; 329:1078-1081.
37. Abmayr SM, Pavlath GK. Myoblast fusion: lessons from flies and mice. *Development* 2012; 139:641-656.

Figure captions:

**Fig.1.** HELPc structure and hydrogels characterization. a) The HELPc backbone is composed of cross-linking (dark gray) and hydrophobic (white) domains repeated eight times. The aminoacid sequence of the monomeric unit (boxed) is reported. A His-tag sequence is located at the N-terminal portion (black). HELPc was obtained by fusing a 41aa sequence from the  $\alpha 2$  chain of the type IV collagen (light gray) at the C-terminus of HELP. The two RGD motifs of the sequence are highlighted in bold. b) Dependence of the storage ( $G'$ ; filled symbols) and loss ( $G''$  open symbols) moduli from the pulsation ( $\omega = 2\pi\nu$ ) for hydrogels composed of HELPc at 7 % (circles) and at 5 % (squares), respectively. c) SEM micrographs of freeze-dried HELPc matrices at different magnifications.

**Fig.2.** Immunofluorescence and morphometric analysis of cells. C2C12 cells were allowed to spread for 5h after seeding on HELPc coated coverslips (Hcc) or on 5% and 7% HELPc gels. (a) Immunofluorescence labeled vinculin. For morphometric analysis at least 100 cells in 10 different microscope fields ( $344 \times 244 \mu\text{m}$ ) were analyzed per condition. To characterize cell morphology, aspect ratio (b, d, f) and cell area (c, e, g) were quantified with ImageJ software. The results are collected from three independent experiments.

**Fig.3.** Immunofluorescence of cytoskeleton and focal adhesions. C2C12 cells were allowed to spread for 5h after seeding on HELPc coated coverslips (Hcc) or on 5% and 7% HELPc gels. F-actin was labeled with Alexa Fluor 594 phalloidin, immunofluorescence labeled vinculin. The results are representative of three independent experiments.

**Fig.4.** Cell viability and proliferation. C2C12 cells were cultured for 5, 24, 48 and 72h on HELPc coated coverslips (Hcc) or on 5% and 7% HELPc gels. At 48h, GM was replaced with DM to start differentiation. a) Average number of nuclei at different time points. Samples were fixed and processed for nuclei staining with DAPI. At least 10 images were taken from each sample under



fluorescence microscope and nuclei were counted with ImageJ software. b) For each condition, the number of nuclei was normalized to the initial nuclei density. Results of three independent experiments done in triplicate. c) WST-1 assay of cells metabolic activity. d) For each condition, the WST-1 values were normalized to the optical density measured at 5h. Results of three independent experiments done in duplicate. \*\*  $p < 0.01$ ; \*\*\*  $p < 0.001$ .

**Fig.5.** Myotubes differentiation. C2C12 cells were plated on HELPc coated coverslips (Hcc) or on 5% and 7% HELPc gels. After 48h proliferation in GM, the medium was changed to DM and the cells were allowed to differentiate. a) Phase contrast micrographs showing myotubes developed on different substrates at 5 days of differentiation. b) Immunofluorescence, performed at 5 days of differentiation, labeled for Myosin Heavy Chain (MHC), while DAPI counterstained nuclei. For the quantitative analysis, at least 900 cells in 12 microscope fields ( $344 \times 244 \mu\text{m}$ ) were analyzed per condition. Differentiation was quantified (c) by calculating the fusion index and (d) by counting the number of nuclei per myotube. Results of three independent experiments. \*\*\*  $p < 0.001$ .

**Fig.6.** Myotubes morphometric analysis. C2C12 cells were plated on HELPc coated coverslips (Hcc) (a, b) or on 5% (c, d) and 7% (e, f) HELPc gels. After 48h proliferation in GM, the medium was changed to DM and the cells were allowed to differentiate for 5 days and processed for MHC immunofluorescence. For the quantitative evaluation, at least 100 MHC-positive myotubes in 10 different microscope fields ( $344 \times 244 \mu\text{m}$ ) were analyzed per condition. Myotube length (a, c, e), and width (b, d, f) were measured with ImageJ software.

**Supplemental Fig.1.** HELPc hydrogel properties. a) HELPc cross-linked hydrogels, polymerized onto glass coverslips; b) 5% and 7% hydrogels casted in cylindrical molds; c) Phase contrast micrographs of HELPc hydrogels; d) AFM characterization of HELPc gels morphology. Surface

height is coded as differences in grey levels as indicated by the altimetric scale in nm (right): lighter parts of the image correspond to higher areas while darker regions are lower in topography.

Fig.1 HELPc structure and hydrogel characterization

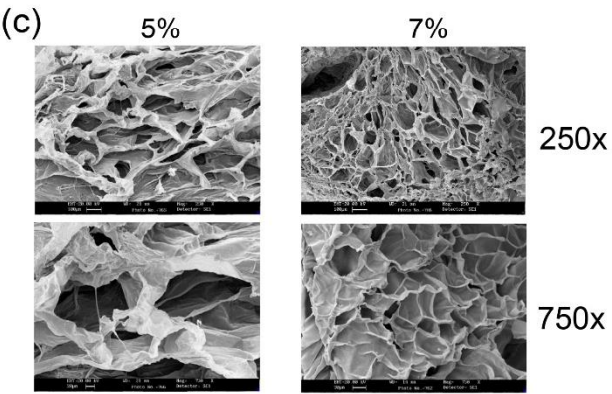
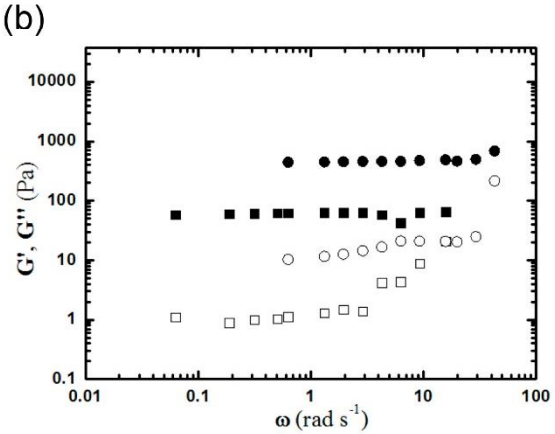
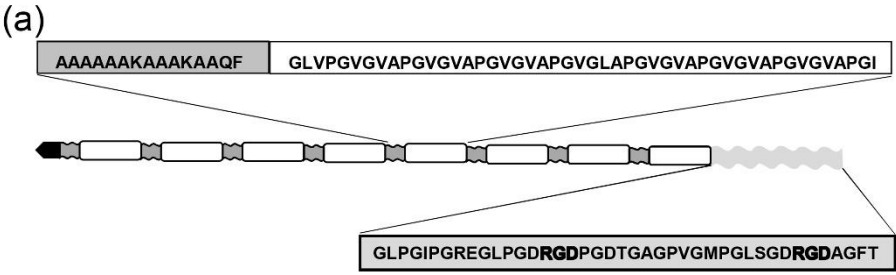


Fig.2 Immunofluorescence and morphometric analysis of C2C12 cells

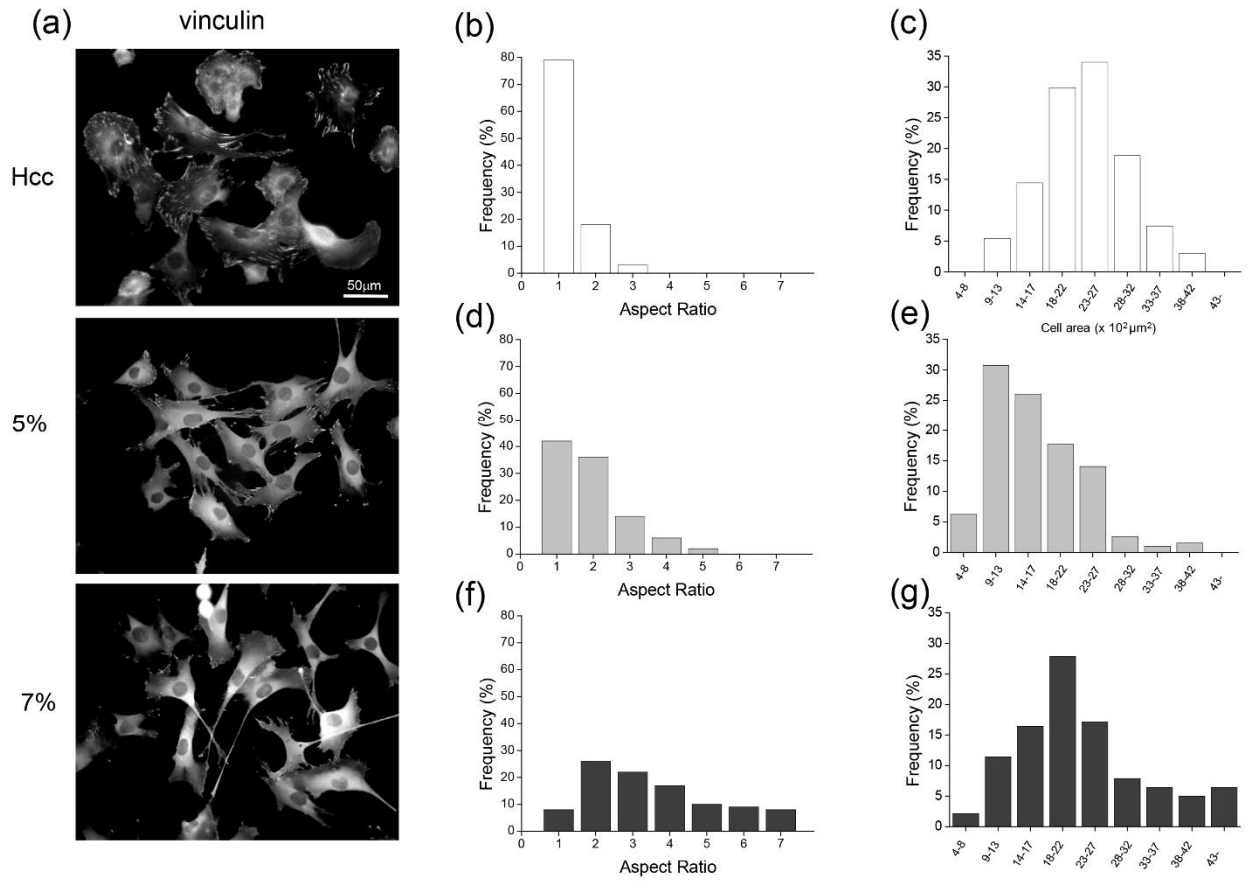


Fig.3 Actin cytoskeleton and focal adhesions

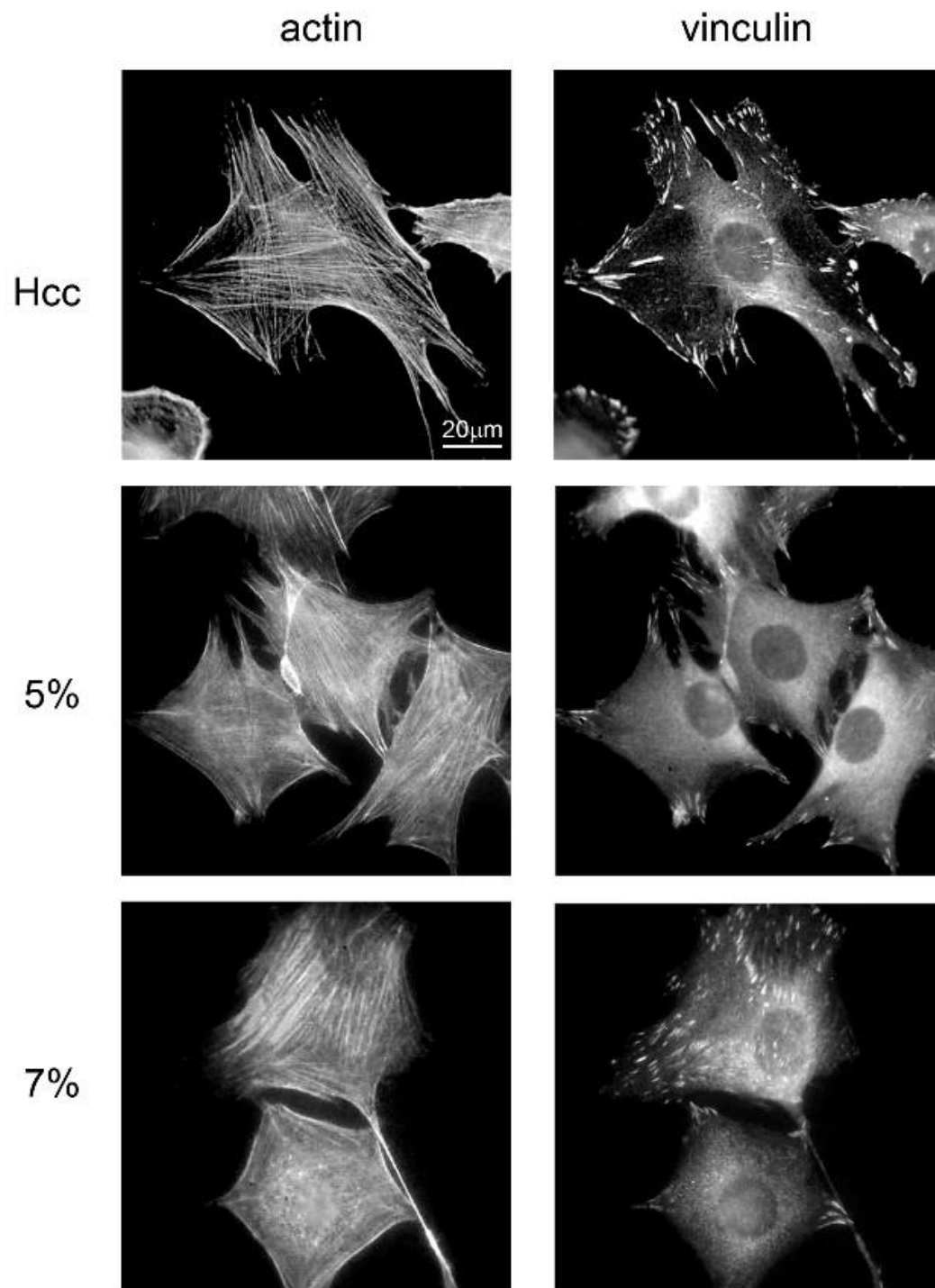


Fig.4 Cell viability and proliferation

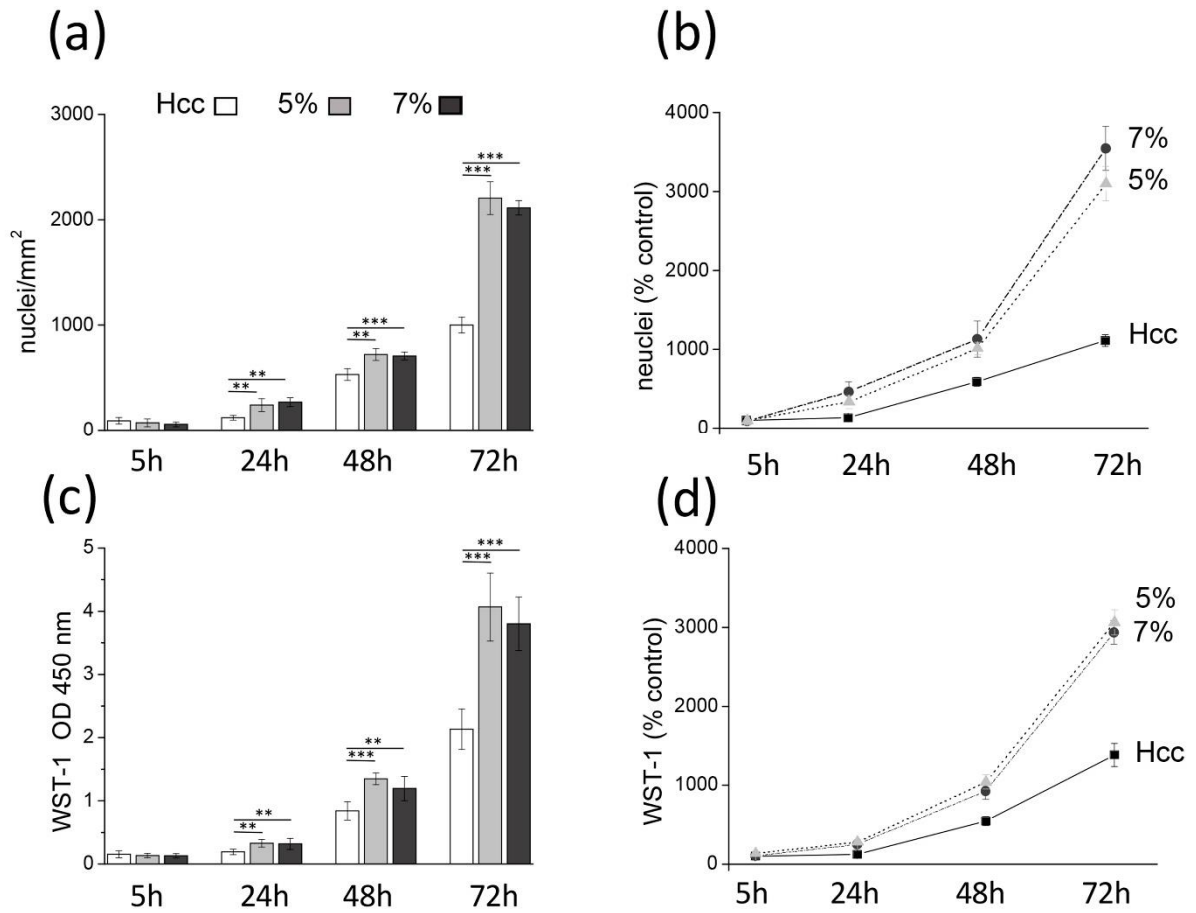


Fig.5 Myotubes differentiation

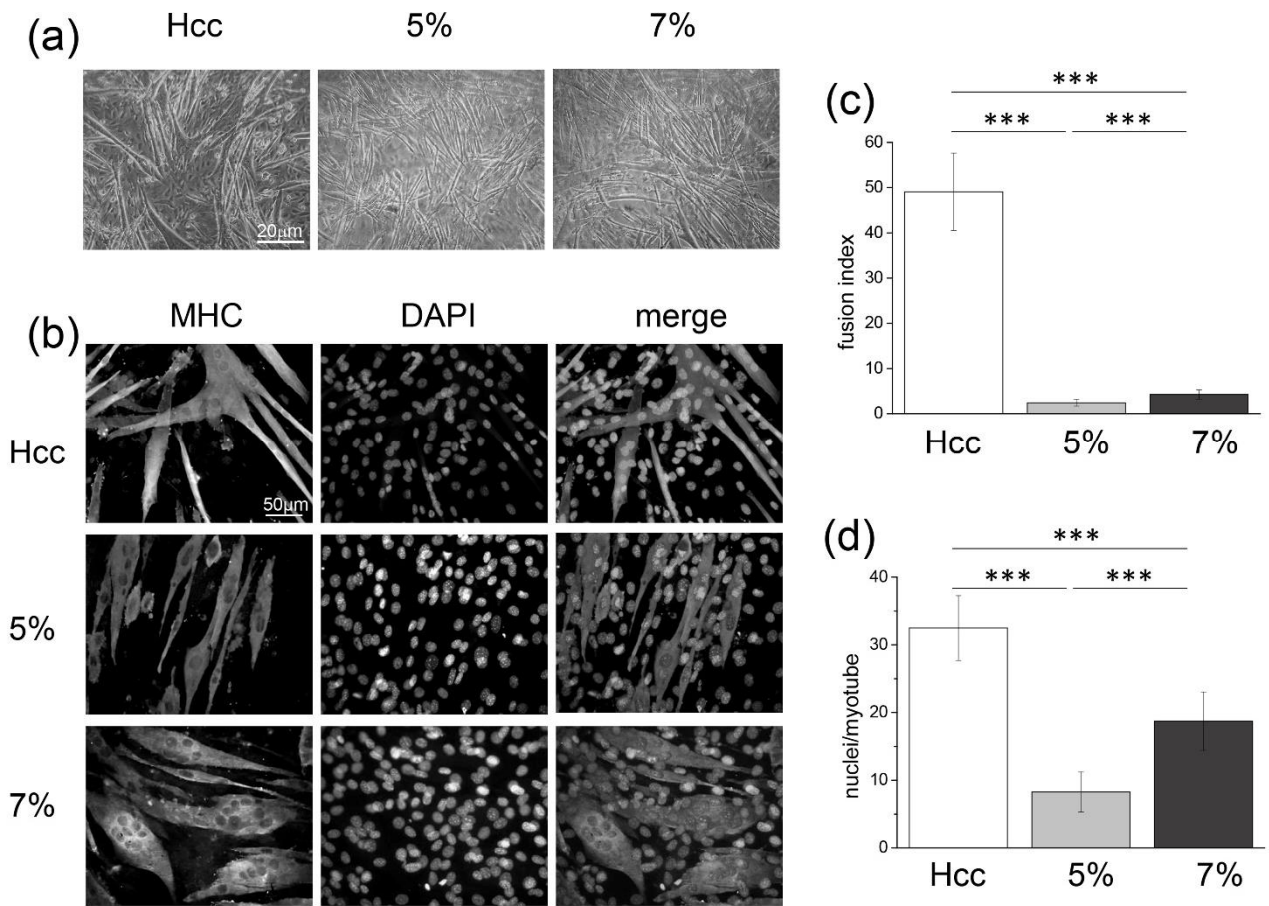
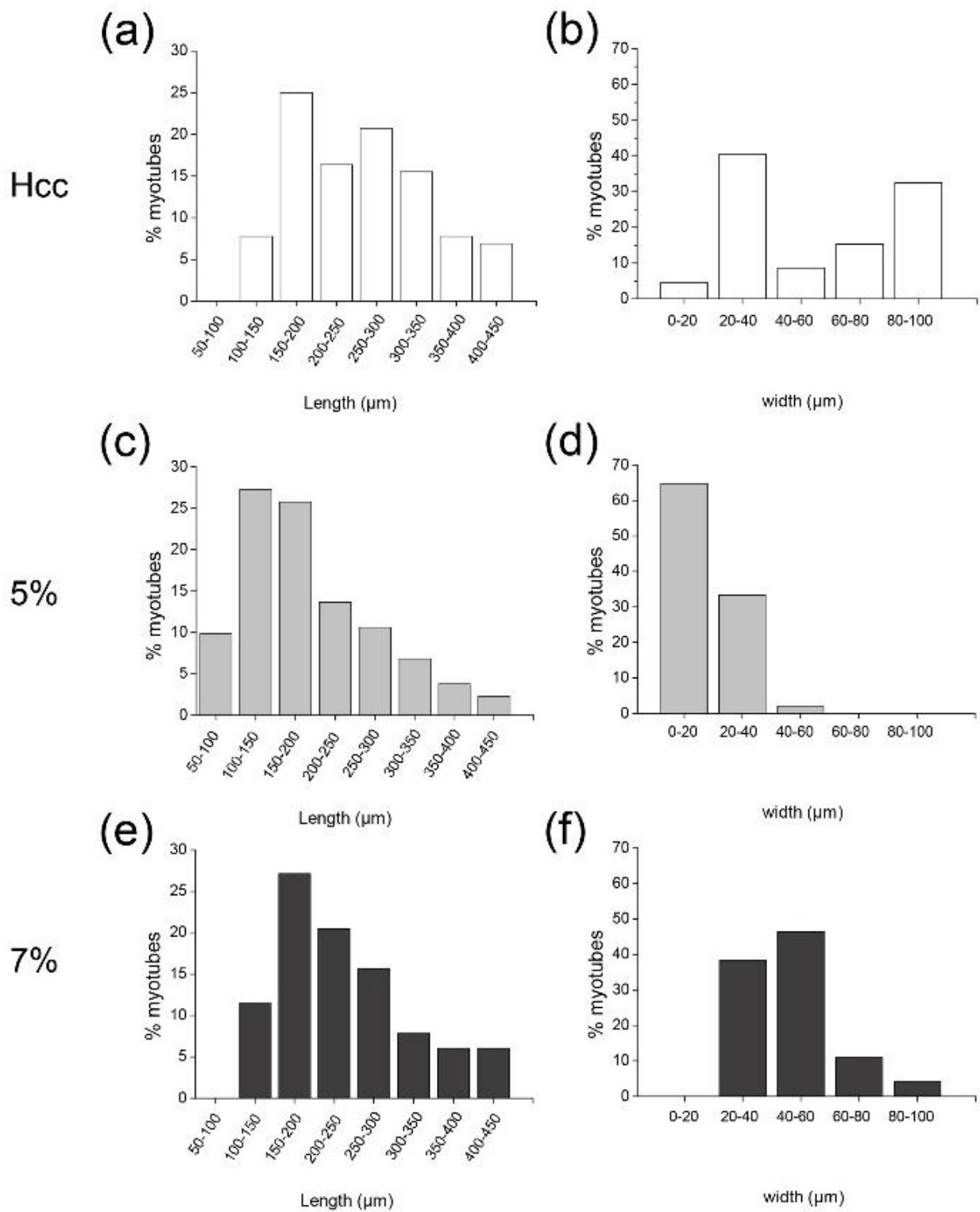


Fig.6 Myotubes morphometric analysis





Supplemental Fig.1: HELPc hydrogel properties

